Scaling of suction-induced flows in bluegill: morphological and kinematic predictors for the ontogeny of feeding performance

Roi Holzman[1,*], David C. Collar[1,2], Steven W. Day[3], Kristin L. Bishop[1] and Peter C. Wainwright[1]

[1]Section of Evolution and Ecology, University of California, One Shields Avenue, Davis, CA 95616, USA, [2]Department of Organismic and Evolutionary Biology, Harvard University, 26 Oxford Street, Cambridge, MA 02138, USA and [3]Department of Mechanical Engineering, Rochester Institute of Technology, 76 Lomb Memorial Drive, Rochester, NY 14623-5604, USA

*Author for correspondence (e-mail: raholzman@ucdavis.edu)

SUMMARY

During ontogeny, animals undergo changes in size and shape that result in shifts in performance, behavior and resource use. These ontogenetic changes provide an opportunity to test hypotheses about how the growth of structures affects biological functions. In the present study, we ask how ontogenetic changes in skull biomechanics affect the ability of bluegill sunfish, a high-performance suction feeder, to produce flow speeds and accelerations during suction feeding. The flow of water in front of the mouth was measured directly for fish ranging from young-of-year to large adults, using digital particle imaging velocimetry (DPIV). As bluegill size increased, the magnitude of peak flow speed they produced increased, and the effective suction distance increased because of increasing mouth size. However, throughout the size range, the timing of peak fluid speed remained unchanged, and flow was constrained to approximately one gape distance from the mouth. The observed scaling relationships between standard length and peak flow speed conformed to expectations derived from two biomechanical models, one based on morphological potential to produce suction pressure (the Suction Index model) and the other derived from a combination of morphological and kinematic variables (the Expanding Cone model). The success of these models in qualitatively predicting the observed allometry of induced flow speed reveals that the scaling of cranial morphology underlies the scaling of suction performance in bluegill.

Key words: biomechanics, ontogeny, scaling, suction feeding, hydrodynamics.

INTRODUCTION

During ontogeny, animals change in size and shape (Brown and West, 2000; Hendriks, 1999; Herrel et al., 2005; Peters, 1983). Frequently, these morphological changes are associated with shifts in function, behavior and resource use. For example, many freshwater fish undergo habitat shifts from densely vegetated littoral zones to more exposed habitats as they grow, and they develop structures and behaviors suitable to avoid predation and capture new prey (Mittelbach, 1981; Mittelbach, 1984; Werner et al., 1983). A major goal in organismal biology is to understand how these ontogenetic changes relate to one another, and the scaling of organismal performance has been instrumental in elucidating the mechanistic links between the changes in form, function and ecology that occur as organisms grow (e.g. Biewener, 1983; Drucker and Jensen, 1996; Hendriks, 1999; Herrel et al., 2005; Peters, 1983). In the present study, we investigate the scaling of suction-induced flow speed and acceleration, two metrics of suction feeding performance in fishes that connect the intrinsic capacity for mouth cavity expansion to the forces exerted on prey (Carroll et al., 2004; Higham et al., 2006a; Holzman et al., 2007; Muller et al., 1982).

Suction feeding fishes generate a flow of water into the mouth by executing a well-coordinated series of cranial movements (Lauder, 1980; Wainwright et al., 2007; Westneat, 2006). Contraction of cranial muscles is translated through a series of joints and levers to an explosive expansion of the intra-oral (buccal) cavity, resulting in a sharp drop in pressure inside the buccal cavity and an acceleration of water into the mouth (Lauder,

1980; Muller et al., 1982; Wainwright et al., 2007; Westneat, 2006). The scaling of the steps in this series of events can be studied, and the observed changes in the musculoskeletal system can be used to generate predictions of the hydrodynamic results. Indeed, aquatic suction feeding has proven a rewarding framework to investigate the scaling relationships between cranial functional morphology and performance (Herrel et al., 2005; Van Wassenbergh et al., 2005; Wainwright and Richard, 1995; Wainwright and Shaw, 1999).

In Table 1 we summarize the results of previous studies of scaling in various aspects of fish suction feeding performance and the underlying morphology. Although a general trend exists between increases in size, mouth-opening leverage and strike duration, the amount of time a strike takes does not describe the effect the fish has on the fluid in front of its mouth. Looking across studies, no general scaling relationship emerges for suction pressure, which is likely to be a result of inter-specific differences in scaling of the transmission of muscle force to buccal expansion and of buccal cavity dimensions (Carroll et al., 2004; Wainwright et al., 2007). Suction pressure is associated with induced flow velocities and accelerations (Higham et al., 2006b; Muller et al., 1982) but the highly unsteady nature of the suction flow regime means that pressure is an indirect measure of the effect of buccal expansion on the surrounding fluid. Data on the scaling of flow speed is limited to that derived from quantitative models, which indicate that simulated flow speed at the mouth decreases with increasing cranial length in one species of catfish (Van Wassenbergh et al., 2006b).

Table 1. Comparison of scaling of suction morphology, kinematics and buccal pressure to standard length (or cranial length) based on published reports in five fish species

Species	Morphology	Strike duration	Pressure
Largemouth bass	Decreasing lever arm ratio of lower jaw with size[1]	Increasing with size[1]	No significant trend[2]
Bluegill sunfish	Decreasing lever arm ratio of lower jaw with size[3]	Increasing with size[3]	Decreasing with size[2]
Spotted sunfish	Decreasing lever arm ratio of lower jaw with size[3]	Increasing with size[3]	No significant trend[2,4]
African catfish	Isometric growth of lever arm ratio of lower jaw and positive allometry of muscle cross-section with size[5]	Increasing with size[6]	Mean pressure decreasing with size (marginally significant)[7]
Snook	Isometric growth of sternohyoideus muscle and buccal cavity area[8]		No significant trend[8]

[1](Richard and Wainwright, 1995); [2](Carroll et al., 2004); [3](Wainwright and Shaw, 1999); [4]Narrow size range and small sample size; [5](Herrel et al., 2005); [6](Van Wassenbergh et al., 2005); [7](Van Wassenbergh et al., 2006b); [8](Wainwright et al., 2006).

Despite these advances in our understanding of the scaling of cranial form and intrinsic performance (e.g. strike duration, suction pressure), no study has empirically measured the scaling of flow speed.

The objective of our present study was to characterize the scaling of the induced flow field during suction feeding in bluegill sunfish, *Lepomis macrochirus* (Rafinesque 1819). Specifically, we ask: (1) is there a relationship between body size and the spatio-temporal patterns of flow in front of the mouth; (2) what is the scaling of peak flow speed in bluegill; and (3) does the observed scaling relationship conform to expectations based on biomechanical models? Direct measurements of the flow in front of the mouth were made using digital particle image velocimetry (DPIV) for fish ranging in size from young-of-year to full-grown, large adults. We focus on the bluegill to build on previous flow visualization and feeding performance studies involving intermediate-sized individuals of this species (Carroll et al., 2004; Day et al., 2005; Higham et al., 2006a; Higham et al., 2006b). Moreover, bluegill are known to be morphologically specialized, high-performance suction feeders that rely on high velocity flows to capture their prey (Carroll et al., 2004; Holzman et al., 2007), and the scaling of flow speed is likely to be relevant to the ontogeny of its feeding ecology.

MATERIALS AND METHODS
Fish were caught locally in Yolo County, near Davis, CA, USA, and housed in 100-liter aquaria at 22°C. The fish were fed daily with pieces of squid (*Loligo* spp.), live ghost shrimps (*Palaemonetes* spp.) and annelid worms. The fish were allowed to acclimate to the experimental aquaria and were trained to feed in the laser sheet (see below) for at least a week before experiments began. Our study included nine individuals (Standard Length=57, 60, 81, 85, 88, 147, 150, 180 and 190 mm), ranging from young-of-year to full-grown, large adults. The experiments described below complied with IACUC approved guidelines for the use and care of animals in research at the University of California, Davis.

Experimental protocol
Fish were starved for 24 h prior to each experiment. At the onset of each feeding trial, the fish was kept in a holding area that was separated from the feeding arena by a sliding door. When the door was opened, the fish was permitted to move across the aquarium and capture its prey. The position and width of the door ensured that the fish approached the prey horizontally, at a right angle to a video camera. The prey (segments of ghost shrimp) were attached to a thin metal wire and held within the laser sheet. Prey size was adjusted to the fish's size and was approximately $\frac{1}{4}$ gape in maximal diameter.

Digital particle image velocimetry
Digital particle image velocimetry (DPIV) was used to quantify water motion in front of the fish's mouth during feeding strikes. The details of this method, as well as the experimental protocol, are described elsewhere (Day et al., 2005; Raffel et al., 1998) and are therefore described here only briefly. An Innova I-90 5 W Argon-Ion continuous wave laser (Coherent, Inc., Santa Clara, CA, USA) was used with a set of lenses and mirrors to produce a vertical laser sheet in the experimental aquarium. The laser sheet, approximately 5 cm in width and 1 mm in thickness, was reflected downwards using a mirror hanging above the aquarium to reduce the effect of the feeding fish's shadow [See fig. 1. in Day et al. (Day et al., 2005) and fig. 1. in Higham et al. (Higham et al., 2005)]. To visualize flow, the water was seeded with nearly neutrally buoyant (specific gravity of 1.05), 12 μm silver-coated, hollow glass beads (Potter Industries, Inc., Carlstadt, NJ, USA). Feeding strikes were filmed in lateral view using a high-speed digital video camera (500 frames s^{-1}, NAC Memrecam Ci; Tokyo, Japan) equipped with a 55 mm lens (TEC-55 f/2.8, Computer Optics, Inc., Hudson, NH, USA). The field of view was adjusted according to the size of the fish by positioning the camera at varying distances from the laser sheet. Additionally, a camcorder recording at 30 frames s^{-1} (Sony, Tokyo, Japan) captured anterior views of the striking fish, which were used to verify the orientation and location of the fish within the laser sheet. Sequential images taken during feeding strikes, treated as image pairs, were analyzed using a cross-correlation algorithm in MatPIV (http://www.math.uio.no/~jks/matpiv), a free toolbox for PIV analysis in MATLAB (MathWorks, Inc., Natick, MA, USA). Image pairs were analyzed using a windows shifting technique, starting with 64×64 pixel interrogation areas and ending with 16×16 pixel areas (with 50% overlap) after six passes. The cross-correlation algorithm returned a two-dimensional grid of vertical and horizontal velocities, and the signal-to-noise ratio (SNR) for each image pair was analyzed.

Quantifying the spatial and temporal pattern of flow
Our variable of interest in the analysis was the magnitude of flow speed at a distance of $\frac{1}{2}$ gape from the center of the mouth at each time point. Previous analysis of the spatial pattern of flow in front of the mouth of bluegill indicated that the flow pattern is approximately radially symmetrical about the long axis of the fish (Day et al., 2005). Therefore, we averaged the flow speed over 21 equally spaced points on a radial transect with a diameter of $\frac{1}{2}$ gape, ranging from +50 to –50 deg. from the imaginary line projecting at a right angle to the mouth (Fig. 1A). Velocity values with a SNR value lower than two were omitted (<10% of the cases). The measure of mean fluid velocity at $\frac{1}{2}$ gape distance from the mouth is referred to throughout the paper as 'flow speed'. We define peak flow speed
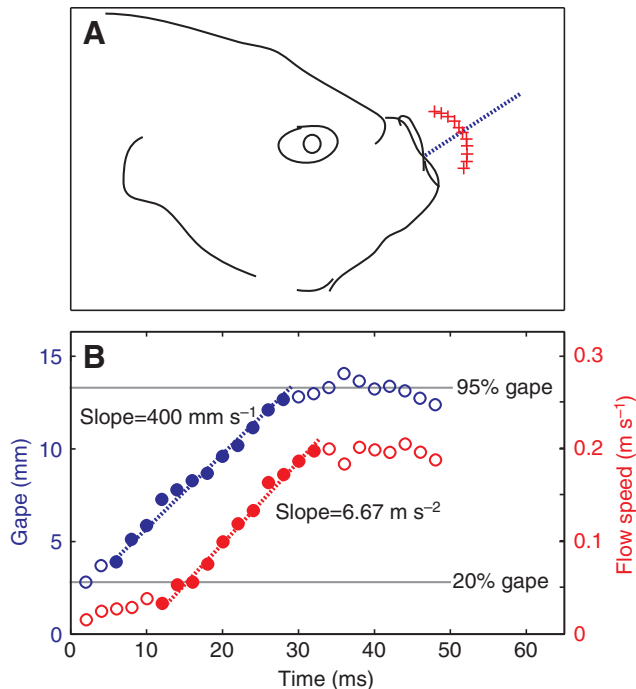
Fig. 1. (A) Sampling locations for flow speed. Flow speeds were averaged over 21 points (red crosses; for clarity only 11 points are shown) equally spaced on a radial transect with a diameter of $\frac{1}{2}$ gape, ranging from +50 to −50 deg. from the imaginary line projecting at a right angle to the mouth. The measure of mean fluid velocity at $\frac{1}{2}$ gape distance from the mouth is referred to throughout the paper as 'flow speed'. Velocity profiles were calculated for points under the imaginary line (broken blue line) projecting at a right angle to the mouth. (B) Determination of time to peak gape (TTPG), linear speed of mouth opening ($\Delta G/\Delta t$) and of the acceleration of the flow in front of the fish's mouth, illustrated on kinematic and flow speed measurements from a typical strike of a 180 mm bluegill sunfish with TTPG=32 ms. For bluegill, the change in jaw angle is constant between strikes (jaw angle transforms from ϕ=10 to ϕ=180), and thus, the time it takes the fish to open its mouth (TTPG; measured from 20% to 95% peak gape; gray reference lines) is inversely proportional to the angular speed of mouth opening, $\Delta\phi/\Delta t$. The linear speed of mouth opening was determined by regression of gape distance on time (dotted blue line) through at least two-thirds of the opening phase of the mouth (filled blue circles). The slope of that regression (400 mm s^{-1}) describes the mean rate of change in gape distance, $\Delta G/\Delta t$, during mouth opening. Fluid acceleration was determined similarly, as the mean rate of change in flow speed over the duration of increasing flow speed (dotted red regression line through closed red circles; 6.67 in this case). We retained strikes for further analysis only if R^2 for the above regression was higher than 0.9.

as the maximum flow speed observed during a strike. Acceleration, defined as the mean change in flow speed as a function of time, was calculated as the least-squares slope for at least four consecutive measurements of flow speed during mouth opening (Fig. 1B). Only slopes spanning at least two-thirds of the mouth opening phase and having an R^2>0.9 were used (>85% of the strikes measured).

Only sequences in which the laser sheet intersected with the mid-sagittal plane of the fish, as verified with the anterior view camera, and in which maximum gape followed prey capture (Day et al., 2005; Higham et al., 2006a) were analysed. In addition to the calculation of flow speed, for each frame, we determined the x and y coordinates of the anterior-most points on the fish's upper and lower jaws, using MATLAB package DLTdataviewer2 (http://www.unc.edu/%7Ethedrick/software1.html). We used these landmarks to calculate gape distance and the angle between the upper and lower jaw (gape angle). For each sequence, we also determined the time to peak gape (TTPG; Fig. 1B), defined as the time it takes the fish to open its mouth from 20% to 95% of the maximal gape observed during the strike (see also Day et al., 2005; Sanford and Wainwright, 2002). We interpreted TTPG as surrogate for the radial speed of mouth opening since it represents the time it takes the jaw to swing from the minimum to maximum angle. We also calculated the linear speed of mouth opening (hereafter $\Delta G/\Delta t$; Fig. 1B) defined as the mean change in dorsal-ventral gape diameter (G) as a function of time (t). Linear mouth opening speed was calculated as the least-squares slope for at least four consecutive measurements of gape distance during mouth opening (Fig. 1B). Only slopes spanning at least two-thirds of the mouth opening phase, and having an R^2>0.9 were used (>95% of the strikes measured). Similarly, we calculated the speed of mouth displacement for each strike, defined as the speed of the mouth center in the earthbound frame of reference. Mouth displacement speed was determined by tracking the center of the mouth for at least four consecutive video frames during mouth opening. An average of 19 strikes was analyzed for each of the nine fish (range from 7 to 30 strikes), each strike consisting of 30–50 frames. Altogether, our study included flow field and kinematic measurements for a total of 170 strikes, corresponding to more than 5400 image pairs.

Previous analysis of the spatial pattern of flow in front of the mouth of bluegill indicated that scaled fluid speed (speed relative to that at $\frac{1}{2}$ gape distance away from the mouth) decreases stereotypically as a function of distance from the mouth [expressed in units of gape distance (Day et al., 2005)]. In the present study, we tested for a relationship between body size and the spatial pattern of flow in front of the mouth. For each fish, we analyzed profiles of fluid speed as a function of distance from the mouth. These profiles were taken at arbitrary time points through the gape cycle, usually between 50% and 150% of TTPG. Profiles were obtained by calculating fluid speed along a transect extending from the center of the fish's mouth (broken blue line in Fig. 1A), oriented at a right angle to the plane of the open mouth (see also Day et al., 2005). Since gape size and peak flow speeds varied between individuals and strikes, we scaled the fluid speed at each point along the transect to $\frac{1}{2}$ gape distance away from the mouth and scaled distance by gape size (see Day et al., 2005). For each of the nine fish, we analyzed profiles from nine randomly selected strikes (total N=81 profiles). We also compared the observed velocity profiles with those based on a fluid-dynamic model [eqn 25 in Muller et al. (Muller et al., 1982)] and with the consensus profile reported by Day et al. [eqn 1 in (Day et al., 2005) based on multiple measurements for three individuals]. This comparison was made by regressing scaled fluid speeds (observed speed divided by that at $\frac{1}{2}$ gape distance from the mouth) against the expected speeds, calculated for the same scaled distance. The velocity profiles for speed at the centerline, based on the fluid-dynamic model (Muller et al., 1982), are expected to follow the equation:

$$U'_x = \frac{-K(G_{rad})^2}{2\sqrt{(x^2 + G_{rad}^2)^3}} \, , \qquad (1)$$

where U'_x is the scaled speed at a distance x from the mouth, G_{rad} is the radius of the gape and K is the speed at the aperture (set to $3.2\times$ the speed at $\frac{1}{2}$ gape distance from the mouth). Empirical results (Day et al., 2005) were best described by the quadratic regression:

$$U'_x = 0.348x^4 - 2.49x^3 + 6.61x^2 - 7.78x + 3.56 \, . \qquad (2)$$

Previous analysis of the temporal pattern of flow indicated that peak flow speed (the maximal flow speed measured through the

sequence) occurred, on average, at 95% of TTPG [with 0% being the time when gape=20% of peak gape, and 100% being the time when gape=95% of peak gape (Day et al., 2005)]. We repeated this analysis in the present study to ask what the time of peak flow speed is for each individual and whether it scales with body size.

Generating predictions of flow speed scaling from biomechanical models

We generated predictions for the scaling of flow speed by estimating the scaling parameters for the morphological and kinematic variables featured in two biomechanical models. The first model, the Expanding Cone model developed by Muller et al. (Muller et al., 1982), is based on the law of continuity, where the physical dimensions of the buccal cavity are expected to determine the flow of water into the mouth. In its simplest form, where the mouth is modeled as a rapidly expanding truncated cone, instantaneous flow speed at the mouth (U) at any time t during expansion is:

$$U_t = -\frac{1}{G_{area}} \int_0^x \frac{\partial B_{area}}{\partial t} \, dB_{length} \, , \qquad (3)$$

where G_{area} is the area of the gape aperture, and B_{area} is the buccal cross-sectional area integrated over the anterior–posterior buccal length B_{length} [based on eqn 18 in Muller et al. (Muller et al.,1982)]. This model predicts that the scaling of flow speed will be a function of the scaling of gape area, buccal cavity length (both affecting buccal volume) and the rate of buccal expansion.

We also compared the scaling of flow speed with the expected scaling based on a model that predicts the morphological potential of a fish to produce suction pressure [Suction Index (SI) (Carroll et al., 2004)] as a function of the transmission of force from the epaxial muscles (proportional to the cross-sectional area of that muscle, A_e) to elevate the cranium and expand the buccal cavity:

$$SI = \frac{A_e \times (L_{in}/L_{out})}{B_{area}} \, , \qquad (4)$$

where L_{in} is the length of the moment arm for the epaxial muscles and L_{out} is the moment arm for the force due to the buccal pressure drop (Carroll et al., 2004). Based on a steady flow mechanics, buccal pressure is expected to be linked to the velocity of the induced flow (Higham et al., 2006b; Muller et al., 1982; Van Wassenbergh et al., 2006b); in fact, a recent study demonstrated that the magnitude of peak negative buccal pressure and peak external flow speeds are correlated (Higham et al., 2006b). Therefore, the scaling of SI and its underlying morphological components can be used to make predictions about the scaling of flow speed. Whereas the Expanding Cone model requires data on both kinematics and morphology to deduce the scaling of flow speed (Van Wassenbergh et al., 2006b), the Suction Index model is based on morphology alone (Carroll et al., 2004).

Measurements for each of the morphological variables featured in the Expanding Cone and Suction Index models were obtained in order to generate predictions about the scaling of flow speed. Morphological measurements were made for eight of the nine individuals used in the flow visualization feeding trials, as well as for three additional individuals (overall N=11). For the ninth fish, we estimated SI, buccal length and morphological gape based on the relationships observed for the 11 other individuals (R^2>0.8 in all cases). To obtain morphological measurements, fish were euthanized after the experiments by overdose of MS-222, fixed in 10% formalin and cleared using trypsin, and then double stained

in Alcian Blue cartilage stain and Alizarin Red bone stain (Taylor, 1967). All measurements were made on freshly dead fish and repeated on cleared and stained specimens to verify accurate identification of relevant anatomical landmarks. We measured morphological gape width (the distance between the left and right coronoid processes of the mandible) buccal length, cross-sectional area of the epaxial muscles, and the lengths of the in- and out-levers of the epaxial muscles. Details of measurement methods have been published previously (Collar and Wainwright, 2006). We used these measurements to calculate each fish's SI according to eqn 4.

To calculate the expected peak flow speed based on the Expanding Cone model we used the measurements of morphological gape and buccal length described above. Dimensions of the posterior buccal diameter were fitted to each individual based on the ratio of posterior-to-anterior diameters in bluegill, measured from silicon molds of the expanded buccal cavity (D.C.C., our unpublished data; N=12 casts, gape size 6–18 mm). The rate of buccal expansion was equated to the mean rate of gape expansion ($\Delta G/\Delta t$), and was kept proportional for the anterior and posterior diameters of the expanding cone, such that the two profiles expanded in synchrony.

Statistical analysis

To assess the relationship between body size and flow patterns (timing of peak flow speed, the slope describing the decay of fluid speed with distance from the mouth and peak flow speed), we regressed log-transformed values of these metrics against the log-transformed standard length of individuals. For each fish (N=9), we used the mean or maximum performance measured, as repeated samples from an individual are non-independent. Similar analysis was made to assess the scaling of speed of mouth opening, TTPG and measurements of cranial morphology (the latter having only one value per fish).

In the above approach, the use of each individual as a basic 'sampling unit' is straightforward and statistically robust; however, it ignores potentially informative within-individual variation. To assess the correspondence between TTPG and peak flow speed (where variation is expected both between and within individuals), we used a mixed model approach (Pinheiro and Bates, 2000). The simplest model included TTPG (independent variable) and peak flow speed (dependent variable), with fish as a random factor. While this model should account for the dependence of the samples within each individual (Pinheiro and Bates, 2000), errors within each individual can still be correlated (e.g. error correlated with observation order). To test for the possibility of correlated errors within dependent samples, we built a series of models of increasing complexity and selected the best model based on the AIC (Akaike information criterion) score and a likelihood ratio test (Johnson and Omland, 2004; Pinheiro and Bates, 2000). These more complex models included a correlation structure for observation order, autocorrelated error and error correlated with the independent variable. In all analyses, the model providing the highest explanatory power included an error correlated with the independent variable (indicating larger error for higher values of flow speed). The results of this latter model are given below.

Similar analyses were used to assess the correlations between $\Delta G/\Delta t$ and peak flow speed, between $\Delta G/\Delta t$ and acceleration, and between peak flow speed and acceleration. In addition, we applied mixed-effects models to evaluate the concordance between the observed profiles and those expected based on the empirical measurements of Day et al. (Day et al., 2005) and those based on theory (Muller et al., 1982). The latter analysis was made by

regressing observed fluid speeds against those expected at the same scaled distance from the mouth.

In analyses where significant effects were found, we calculated the coefficient of determination (R^2) based on the log-likelihood results of the model using the equation:

$$R^2 = 1 - \exp\left(-\frac{2}{N}(\log L_m - \log L_0)\right), \qquad (5)$$

where N is the number of observations, $\log L_m$ is the log-likelihood of the model of interest, and $\log L_0$ is that of an intercept-only model (Magee, 1990). Statistical analyses were done using the free software R statistics (v. 2.5.0; http://www.R-project.org), after verifying normal distribution of residuals for mixed effects models and regression analysis.

RESULTS
Scaling of the Suction Index model

Under isometric growth of the elements in the model, the SI should not change with standard length, resulting in a scaling exponent of 0. However, the SI of *Lepomis macrochirus* increases with strong positive allometry (linear regression on log-transformed values; $R^2=0.82$, $F_{1,9}=38.72$, $P<0.001$, slope=1.1 ± 0.17; Fig. 2B; Table 2). The lever ratio for cranial elevation (L_{in}/L_{out}) increased with positive allometry (linear regression on log-transformed values; $R^2=0.67$, $F_{1,9}=16.7$, $P<0.015$, slope=0.57 ± 0.13; Fig. 2C). This trend was complimented by positive allometry in the growth of cross-sectional area of the epaxial muscle (a proxy for the force capacity of that muscle; linear regression on log-transformed values; $R^2=0.98$, $F_{1,9}=669$, $P<0.001$, slope=2.7 ± 0.1; Fig. 2D). However, increase in buccal area (inversely related to SI) with body size did not differ

from isometry (linear regression on log-transformed values; $R^2=0.91$, $F_{1,9}=84.4$, $P<0.001$, slope=2.16 ± 0.23). The observed scaling of SI led to the prediction that flow speed should increase with standard length with a slope of 0.55, as pressure is expected to scale with flow speed squared under conditions of steady flow.

Scaling of the Expanding Cone model

There was considerable variation in TTPG both between and within individuals in this study. Within individuals, maximal TTPG (range 20–66 ms) was 2.5–3.5-fold longer than the minimal TTPG (range 6–20 ms). Between individuals, mean TTPG was not significantly correlated with fish standard length (linear regression on log-

Table 2. Scaling of suction performance based on observed flow speed and those predicted based on the Suction Index model (Carroll et al., 2004) and the Expanding Cone model (Muller et al., 1982).

	Scaling exponent (±s.e.m.)	R^2	F, P value
Suction Index	0.55±0.09	0.82	$F_{1,9}=38.7$ $P<0.001$
Expanding Cone	0.98±0.2	0.76	$F_{1,7}=22.6$ $P<0.001$
Observed flow speed	0.78±0.18	0.72	$F_{1,7}=17.8$ $P<0.005$

Buccal pressure is expected to be proportional to flow speed squared; therefore the predicted scaling exponent for flow speed based on the Suction Index model is 0.55. Scaling exponent for both models was not significantly different from the observed one for flow speed (t-test using slope ± confidence intervals; $P>0.05$ for both). Reported F and P values are for the null hypothesis that slope=0.
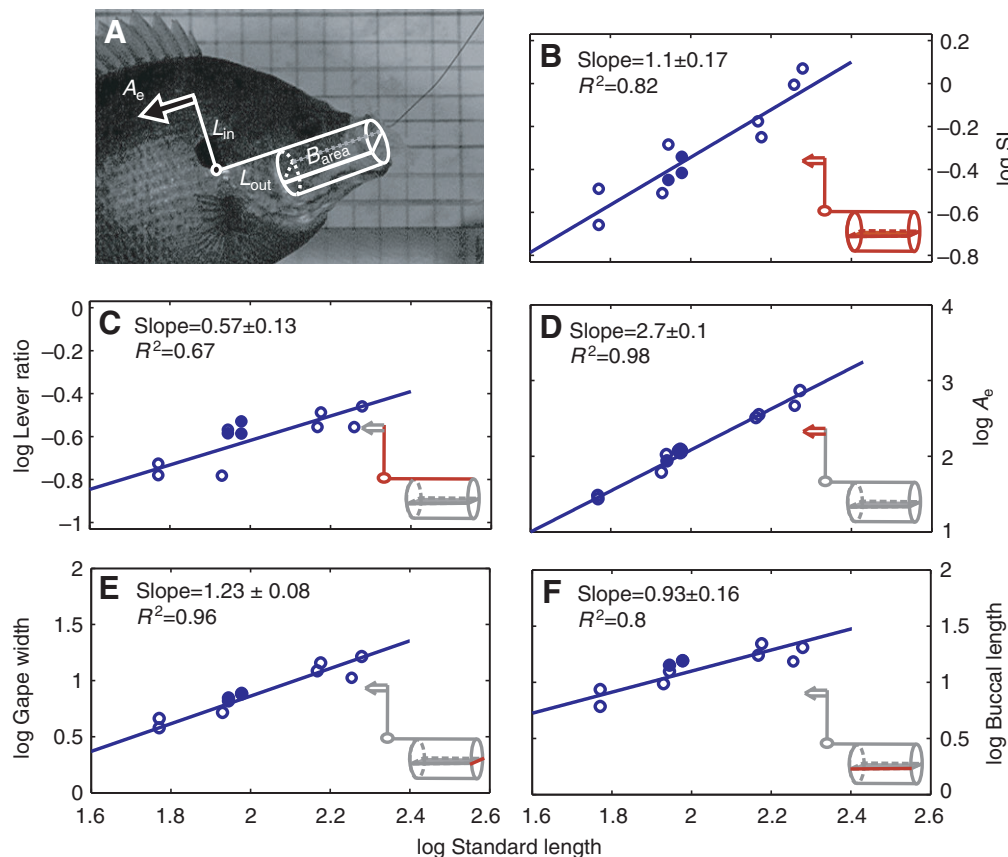

Fig. 2. Scaling of Suction Index (SI) and its underlying morphological components in bluegill, *Lepomis macrochirus*. (A) SI is a morphology-based index that describes the fish's potential to create suction pressure [Carroll et al., 2004; image modified from Collar and Wainwright (Collar and Wainwright, 2006)]. SI (arbitrary units) increases proportionately with the fish's length (B), due to the positive allometry of the lever ratio (C), the positive allometry of the cross-sectional area of the epaxial muscle (mm^2) (D) ,and isometry of the buccal area. Buccal area is calculated based on morphological gape (mm) (E) and buccal length (mm) (F). Morphological gape and buccal length are also used, together with gape kinematics, to predict peak flow speed based on the Expanding Cone model (eqn 3; Fig. 3C). A_e, cross-sectional area of the epaxial muscle; L_{in}, in-lever arm, L_{out}, out-lever arm, B_{area}, buccal area. In the inset for each panel (B–F) the components of SI contributing to the dependent variable (y-axis) are colored red. Data are for N=11 fish (open circles=8 experimental fish; closed circles=3 other specimens).

transformed means; $R^2=0.16$, $F_{1,7}=1.36$, $P>0.28$, slope=0.37 ± 0.32; Fig. 3A). Similarly, the fastest TTPG observed for each individual (an indicator of maximal performance) was not correlated with standard length (linear regression on log-transformed values; $R^2=0.14$, $F_{1,7}=1.18$, $P>0.31$, slope=0.33 ± 0.3; Fig. 3A).

There was high variability in linear speeds of mouth opening, $\Delta G/\Delta t$, within individuals, with a 27-fold difference between fastest and slowest strikes. However, between individuals, $\Delta G/\Delta t$ increased with standard length (linear regression on log-transformed means; $R^2=0.74$, $F_{1,7}=20.7$, $P<0.002$, slope=0.95 ± 0.2; Fig. 3B) from a mean of $0.22\,\mathrm{m\,s^{-1}}$ for the smallest fish (59 mm) to $1.46\,\mathrm{m\,s^{-1}}$ for the 190-mm fish. A similar trend was observed for the fastest $\Delta G/\Delta t$ observed for each individual (linear regression on log-transformed values; $R^2=0.81$, $F_{1,7}=29.7$, $P<0.001$, slope=1.0 ± 0.18; Fig. 3B).

Morphological gape increased with positive allometry (linear regression on log-transformed values; $R^2=0.96$, $F_{1,9}=194$, $P<0.001$, slope=1.23 ± 0.08; Fig. 2E), while the length of the buccal cavity increased isometrically (linear regression on log-transformed values; $R^2=0.8$, $F_{1,9}=33.1$, $P<0.001$, slope=0.93 ± 0.16; Fig. 2F). These morphological measurements, together with the speed of mouth opening, $\Delta G/\Delta t$, were used to parameterize the Expanding Cone model (based on Eqn 3). The observed scaling of the Expanding Cone model indicated that flow speed is expected to increase in proportion with standard length, with a scaling exponent of 0.98 ± 0.2 (linear regression on log-transformed values; $R^2=0.76$, $F_{1,7}=22.6$, $P<0.001$; Fig. 3C; Table 2).

Scaling of closing speed on the prey

In accordance with the use of suction feeding to move the prey towards the mouth, fish employ body ram and jaw protrusion to help decrease the distance on their prey. The mean mouth displacement speed (indicating the closing speed on the prey; defined as the sum of jaw protrusion speed and body ram) increased significantly with standard length (linear regression on log-transformed values; $R^2=0.55$, $F_{1,7}=8.8$, $P<0.02$, slope=0.7 ± 0.23), as did the maximal speed observed for each individual (linear regression on log-transformed values; $R^2=0.52$, $F_{1,7}=7.58$, $P<0.026$, slope=0.6 ± 0.21).

Spatial patterns of flow

As previously indicated (Day et al., 2005), the spatio-temporal pattern of fluid speeds in front of the mouth is primarily dependent on gape and the magnitude of fluid speed at the mouth aperture. These relationships provide the framework for the following analysis, where speeds are scaled for the speed at $\frac{1}{2}$ gape distance away from the mouth (hereafter 'flow speed') and distances are scaled to gape distance.

Regardless of gape size, the flow generated by the suction-feeding fish was restricted to the proximity of the mouth, and the magnitude of fluid speed dropped sharply as a function of the distance from the mouth center. On average, the speed at $\frac{1}{2}$ gape distance away from the mouth was 28% of the speed at the center of the mouth,
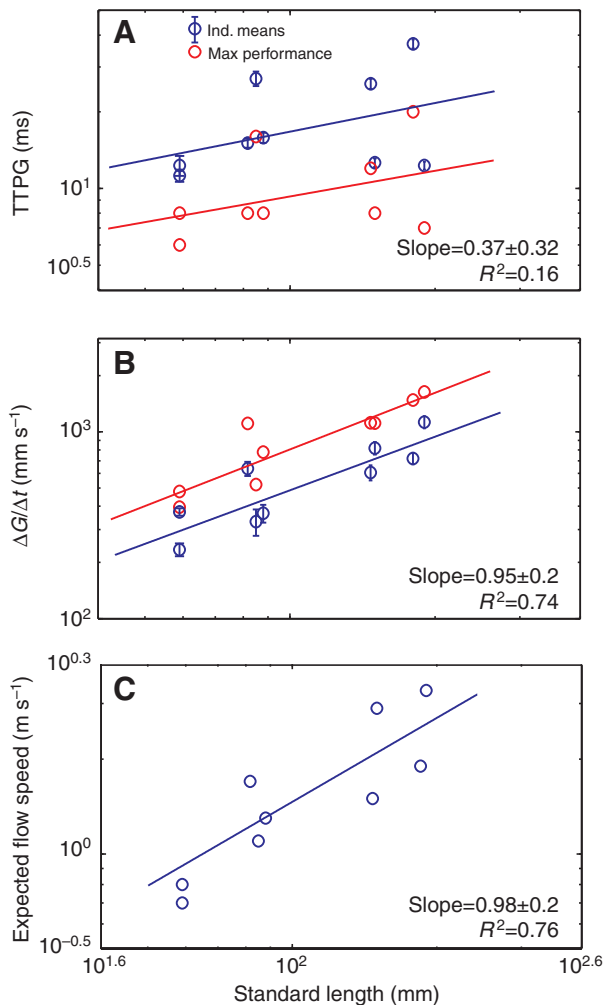

Fig. 3. Scaling of jaw kinematics for suction feeding bluegill, *Lepomis macrochirus*. (A) The time to peak gape (TTPG), defined as the time it took the fish to fully open its mouth (ms), was not significantly correlated with fish length. (B) The linear speed of mouth opening ($\Delta G/\Delta t$) was significantly correlated with standard length, and its scaling exponent was not significantly different from 1. The observed scaling of morphology and kinematics (buccal length, gape size and speed of mouth opening) was used to generate predictions for the scaling of flow speed (C) based on the Expanding Cone model (see eqn 3). Data are means ± s.e.m. (blue circles) or value of fastest speed observed (red circles). Slopes are for the regression of log-transformed mean values and standard length. *N*=9 fish, 7–30 strikes per fish.
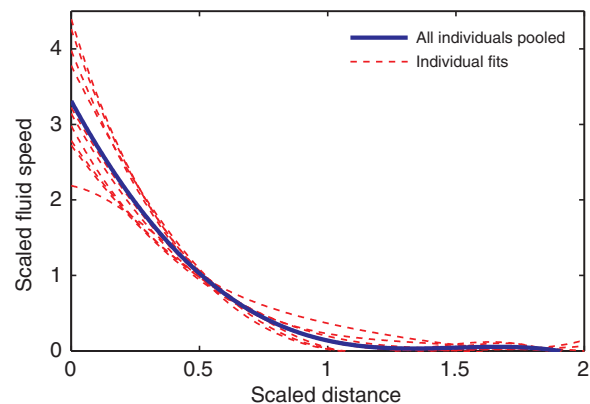

Fig. 4. Mean profiles of scaled fluid speed along the centerline transect for each of the nine individuals (broken red lines), in addition to a polynomial fit for the pooled data set (blue line). The deviations of individual profiles from the mean profile (averaged over all individuals) were small (average residual=3% of the speed at $\frac{1}{2}$ gape±0.7%) and not significantly correlated with size. Scaled fluid speed is fluid speed relative to flow speed at $\frac{1}{2}$ gape distance from the mouth, whereas scaled distance is the distance in gape diameters.

and the speed at 1 gape distance from the mouth was 5% of that at the mouth. This pattern was consistent irrespective of gape size and body length. Velocity profiles at the centerline, representing the scaled speed (relative to the speed at $\frac{1}{2}$ gape distance from the mouth) as a function of scaled distance from the mouth center (expressed in gape diameters) were similar for the different individuals (Fig. 4). The deviations of individual profiles from the mean profile averaged over all individuals were small (average residual=3% of the speed at $\frac{1}{2}$ gape±0.7%) and not correlated with size (linear regression between average residuals and SL; $R^2=0.01$, $F_{1,7}=0.6$, $P>0.8$).

We compared the observed velocity profiles with those based on a fluid-dynamic model (eqn 1) and also with the consensus profile reported in Day et al. (eqn 2). The observed scaled speeds concurred with the expected values generated based on empirical data (Day et al., 2005; mixed effect model; $R^2=0.92$, $F_{1,7}=10193$, $P<0.001$; Slope=0.87±0.055) as well as for those values based on the fluid-dynamic model [(Muller et al., 1982), mixed effect model; $R^2=0.92$, $F_{1,7}=10621$, $P<0.001$; slope=0.99±0.057].

Temporal patterns of flow

In general, the temporal pattern of the flow speed closely followed gape kinematics, regardless of fish size (Fig. 5). Flow speed gradually increased through the gape cycle, reaching a peak just before peak gape. Timing of peak flow speed (the highest flow speed measured in the strike) was variable around a mean of 90% of TTPG (individual means ranging from 78% of gape cycle to 116%) but did not vary systematically with standard length (linear regression on log-transformed values; $R^2=0.001$, $F_{1,7}=0.01$, $P>0.9$, slope=–0.016±0.14; Fig. 6).

Kinematic predictors of flow speed

Within individuals, peak flow speeds associated with slower TTPG were lower than peak flow speeds associated with fast TTPG. However, there was significant inter-individual variation in the strength of the correlation between TTPG and peak flow speed. The average correlation coefficient between TTPG and peak flow speed was $R^2=0.4±0.28$ (range 0.1–0.89; $N=9$ individuals) but there was
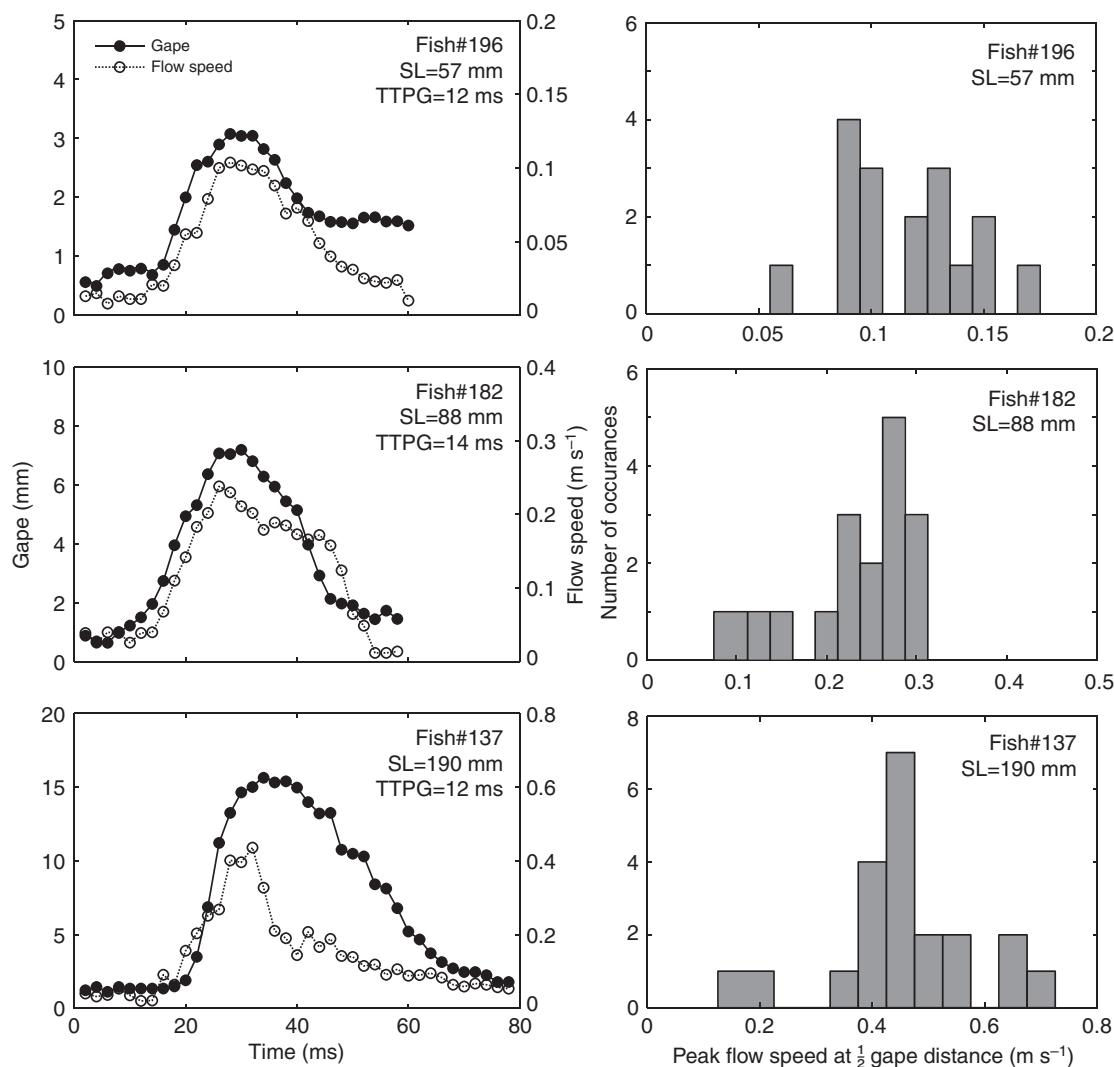

Fig. 5. Representative sequences of gape kinematics (filled circles; solid lines) and flow speed (open circles; dotted lines) as function of time (left column) and histograms of peak flow speeds observed during the experiments (right column). Data are for three individuals representing (from top to bottom) the smallest fish, an intermediate fish, and the largest fish used in this study. Note that the time axis (x-axis in left column) is identical for the three fish however, gape distance and flow speed (y-axes in left column, x-axis on right column) increase with increasing fish size. SL is standard length. TTPG is the time to peak gape.
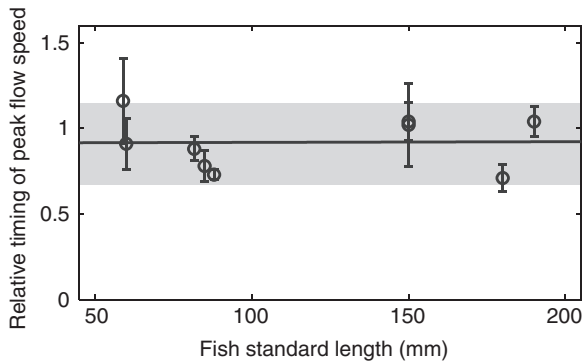
Fig. 6. The relative timing of peak flow speed as a function of standard length. The timing of peak flow speed is expressed in fractions of the time to peak gape (TTPG), such that, at time 0, the gape equals 20% of the maximal gape and, at time 1, gape equals 95% of the maximal gape. The mean (± s.e.m.) relative timing of peak flow speed was 0.92 (±0.05). Data are mean values ± s.e.m. for each fish. The horizontal line (± gray band) represents the mean (± s.d.) timing of peak flow speed reported previously for intermediate sized bluegill (Day et al., 2005).
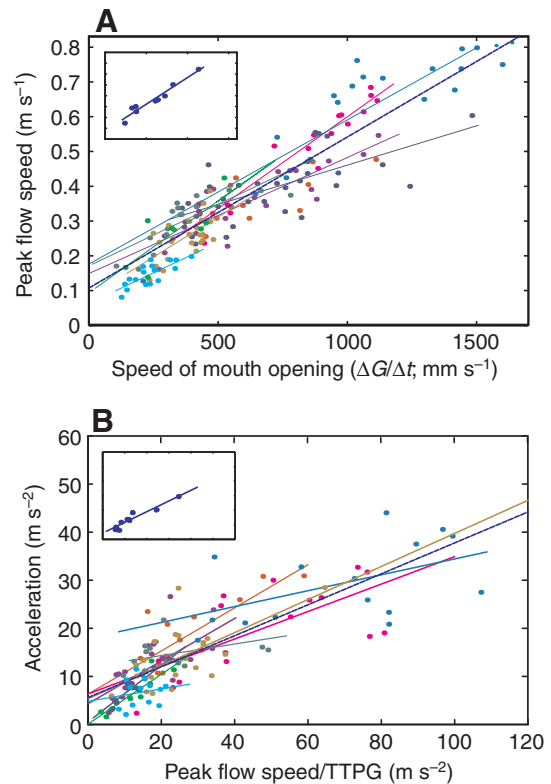

Fig. 7. (A) Peak flow speed at half gape distance from the mouth as a function of $\Delta G/\Delta t$, the linear speed of mouth opening, and (B) acceleration at half gape distance plotted against the ratio of peak flow speed to time to peak gape (TTPG). Different colors represent individual fish (N=9 fish; standard length=57–190 mm) and individual points represent strikes (7–30 strikes per fish). Blue line represents regression for the pooled data set. Insets are for individual means, with x- and y-axes identical to those of the main panels.

no correspondence between the proportion of explained variance and size. As predicted by the Expanding Cone model (Muller et al., 1982) for the same TTPG, the flow speeds measured for smaller fish were lower. A statistical model for the correlation between TTPG and peak flow speed, incorporating both between- and within-individual variation in TTPG explained 28% of the variation in peak flow speed (mixed effect model; $R^2=0.28$, $F_{1,7}=40.3$, $P<0.001$). Therefore, only measuring TTPG was insufficient to explain size-dependent, between-individual variation. However, by incorporating standard length to that model, both TTPG and standard length had a significant effect on peak flow speed, and the model explained 67% of the variation in peak flow speed (mixed effect model; $R^2=0.67$, $P<0.001$ for standard length, $P=0.033$ for TTPG).

In contrast to the effect of TTPG, $\Delta G/\Delta t$ better explained variation in peak flow speed both within and between individuals. Within individuals, the average correlation coefficient between $\Delta G/\Delta t$ and peak flow speed was $R^2=0.61\pm0.16$ (range 0.4–0.9; N=9 individuals). Moreover, $\Delta G/\Delta t$ explained a high proportion of the total variation in peak flow speed. A statistical model for the correlation between $\Delta G/\Delta t$ and peak flow speed, encompassing both within- and between- individual variation in $\Delta G/\Delta t$ explained 72% of the overall variation in peak flow speed (mixed effect model; $R^2=0.72$, $F_{1,7}=387$, $P<0.001$; Fig. 7A). These relationships can be expected based on the Expanding Cone model, assuming that $\Delta G/\Delta t$ reflects the rate of volumetric change in the buccal cavity. In addition, we found no correlation between standard length and the slope of the regression between $\Delta G/\Delta t$ and peak flow speed (linear regression on log-transformed values; $R^2=0.02$, $F_{1,7}=0.11$, $P>0.74$). This similarity in slopes indicates that the nature of translating strike kinematics to external water flow is similar between body sizes.

The kinematics of $\Delta G/\Delta t$ accounts for both the variation in strike duration (because of the Δt component) and for the variation in gape size (because of the ΔG), but these components differ in their response to standard length. To tease out the effect of fish size, we tested the relationship between standard length and the rate of relative gape increase, $\Delta G_r/\Delta t$, (as independent predictors) and peak flow speed, where G_r is defined as relative gape (instantaneous gape/peak gape). Similar to the observed trend with TTPG, both $\Delta G_r/\Delta t$ and standard length had a significant effect on peak flow speed, with the model explaining 65% of the variation in peak flow

speed (mixed effect model; $R^2=0.65$, $P<0.001$ for standard length, $P=0.014$ for $\Delta G_r/\Delta t$).

Accelerations

Fluid acceleration is defined as the temporal change in fluid speed (see Fig. 1B for determination of acceleration) and is expected to correspond to the ratio of peak flow speed (net change in flow speed) to TTPG (the time span in which that change occurred). Indeed, this ratio (peak flow speed/TTPG) was significantly correlated with the magnitude of fluid acceleration at a distance of $\frac{1}{2}$ gape from the mouth (mixed effect model; $R^2=0.42$, $F_{1,7}=29.33$, $P<0.001$) capturing both within and between individual variation (Fig. 7B). Moreover, as $\Delta G/\Delta t$ was a good surrogate for flow speed (Fig. 7A), the ratio of $\Delta G/\Delta t$ to TTPG was also similarly correlated with the magnitude of fluid acceleration (mixed effect model; $R^2=0.40$, $F_{1,7}=26.02$, $P<0.001$).

Scaling of flow speeds and accelerations

Between individuals, peak flow speed increased with standard length (linear regression on log-transformed values; $R^2=0.72$, $F_{1,7}=17.8$, $P<0.003$, slope=0.78±0.18; Fig. 6; Fig. 8A; Table 2). However, the acceleration (measured at $\frac{1}{2}$ gape from the mouth) was not significantly related to standard length (linear regression on log-transformed values; $R^2=0.15$, $F_{1,7}=1.29$, $P>0.29$, slope=0.44±0.38; Fig. 8B). Similar correlations (or lack thereof) were observed for maximal performance (fastest flow and acceleration; Fig. 8).
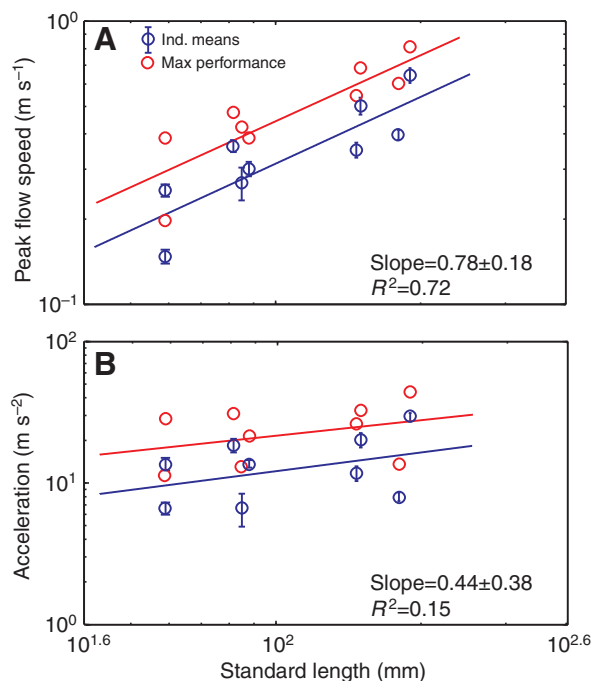
Fig. 8. Scaling of peak flow speed and acceleration at $\frac{1}{2}$ gape distance in bluegill. Peak flow speed increases with size whereas the relationship between acceleration and standard length is not statistically significant. Data are mean values ± s.e.m. (blue circles) or maximal performance strikes (red circles). N=9 fish, 7–30 strikes per fish. Slopes are for the regression of log-transformed mean values and standard length.

DISCUSSION

As bluegill grow, they are capable of inducing faster flows during suction feeding. Using flow visualization, we found that the magnitude of peak flow speed increases with body size (Fig. 8), and the absolute effective suction distance increases due to the absolute increase in gape size. However, the scaled spatial pattern of flow in front of the mouth remains unchanged during ontogeny. Across all body sizes, the decay of flow speed as a function of scaled distance from the mouth was stereotypic in bluegill (Fig. 4). Moreover, the temporal pattern of flow does not change as bluegill grow. The relationships between peak flow speed and TTPG (Fig. 6) and between $\Delta G/\Delta t$, and flow speed (Fig. 7) are similarly strong across the range of body sizes examined in this study. The observed size independence of the scaled spatial and temporal patterns of flow indicate that bluegill do not experience a fundamental change in the way buccal expansion translates to water motion, as might be expected if changes in gape area proportions or opening angle (the occurrence of a 'notched' gape) had occurred (Higham et al., 2006a).

The observed scaling relationships between standard length and peak flow speed generally conform to expectations based on two biomechanical models, the Suction Index model (Carroll et al., 2004) and the Expanding Cone model (Muller et al., 1982). The Suction Index model predicted an increasing relationship (scaling exponent of 1.1±0.17; Fig. 2B) between standard length and capacity to produce suction pressure, which is, to a first approximation, related to peak flow speed squared (resulting in an expected scaling exponent of 0.55 between standard length and flow speed). Scaling of the Expanding Cone model similarly predicted an increasing relationship between standard length and expected peak flow speed but with a scaling exponent of 0.98±0.2 (Fig. 3C; Table 2). These scaling exponents are in general agreement with the observed

relationship between peak flow speed and standard length (scaling exponent of 0.78±0.18; Fig. 8A; Table 2). One reason for the disparity between the predictions of the Suction Index model and the observed scaling relationship is that the model predicts suction pressure rather than flow speed. Although pressure inside the buccal cavity is tightly linked to the velocity of the induced flow, this relationship is not perfect, perhaps due to some effect of unsteady flow (Higham et al., 2006b). A dynamic model of flow and pressure in the buccal cavity could help formulate more robust predictions on the connections between pressure and flow speed. Lastly, the uncertainty in determining SI is higher, since it is evaluated once for each fish whereas the flow speed predicted by the Expanding Cone model is based on the mean for multiple measurements of $\Delta G/\Delta t$ per fish. Nonetheless, the Suction Index model performed well as a predictor of flow speed and has appeal to future studies as it can be applied without the use of hard-to-obtain kinematic data, which can facilitate data acquisition.

Contractile properties of catfish feeding muscles can change during ontogeny, in addition to scaling of the leverage system. In catfish, a significant increase in force per unit cross-sectional area was inferred for the hypaxial muscle with increasing fish size (Van Wassenbergh et al., 2007). Concomitantly, a decrease in muscle-mass-specific power for suction feeding with increasing size was observed (Van Wassenbergh et al., 2005). This suggests a lower suction effort in larger catfish and corresponds with their trend of decreasing buccal pressure with increasing size. However, the Suction Index model assumes suction force to scale proportionally with the cross-sectional area of the epaxial muscle. If the scaling relationships inferred for catfish also apply to the bluegill sunfish, this would further increase the predicted slope by the Suction Index model.

The Expanding Cone model postulates that maximal flow speed will increase in proportion to the length of the buccal cavity, as we observed in the present study (Fig. 3C; Fig. 8A; Table 2). However, this model also predicts that maximum flow velocity occurs at ~66% of peak gape (Muller et al., 1982; van Leeuwen and Muller, 1983), which is much earlier in the strike than the flow velocity observed using flow visualization techniques (see also Day et al., 2005; Ferry-Graham et al., 2003; Higham et al., 2006a). Moreover, flow speeds predicted by the simple Expanding Cone model were approximately six times higher than the observed flow speeds (compare x-axis for Fig. 3C and Fig. 8A). Recent attempts to introduce a time delay between anterior and posterior expansion of the cone, as well as to model the buccal cavity as a series of elliptical cylinders or expanding truncated cones (Bishop et al., in press; Van Wassenbergh et al., 2006a; Van Wassenbergh et al., 2006b) may address these shortcomings. Not withstanding these limitations, the single cone representation of the fish's mouth is apparently sufficient to qualitatively predict the scaling of flow speed within a species.

While both models are limited in their accuracy to quantitatively predict the scaling of flow speed in bluegill, the general agreement between the observed scaling of flow speed and the predictions derived from these biomechanical models demonstrate that growth of cranial structures underlies the ontogenetic changes in flow speed. As the scaling of these structures will vary across species, it is unlikely that any general trend in the scaling of suction performance will be observed across species. For example, in African catfish increases in cranial length are not accompanied by changes in rate of buccal expansion (Van Wassenbergh et al., 2005), ultimately resulting in a (marginally significant) negative relationship between size and the capability to produce flow (Van Wassenbergh et al., 2006b). In largemouth bass, SI does not vary with size (Carroll et

al., 2004), indicating that flow speed should not change during ontogeny. The lack of a general trend in scaling of suction feeding performance across African catfish, largemouth bass, snook and spotted sunfish (Table 1 and references therein) further supports the claim that species-specific scaling of morphology will result in variation in the scaling of suction feeding performance across fish species. In fact, the null hypothesis of isometric growth of cranial features is translated to a scaling exponent of 0 between standard length and SI. It is the positive allometry of cranial morphology in bluegill (Fig. 2) that underlies the increase in flow speeds with increasing size. Note that the observed allometry between standard length and SI is different from the negative allometry reported by Carroll et al. (Carroll et al., 2004). This discrepancy is probably due to the limited range of bluegill body sizes in their experiment, which represents a subset of sizes examined in this study (standard length=130–170 mm compared with 60–190 mm in this study).

The time to open the mouth in the bluegill scales differently from results in a previous study on the same species, which reported a slope of 0.834±0.005 (Wainwright and Shaw, 1999). The difference between the results of the present study and this earlier work is not statistically significant, in part because of noise in the data presented here (low power to detect the true slope). Our analysis of the scaling of strike kinematics indicates that, although TTPG seems to be unrelated to the fish's length, $\Delta G/\Delta t$ strongly correlates with standard length and is a better predictor of peak flow speed than TTPG, accounting for the observed variation both within and between individuals. The poorer performance of TTPG may be due to its determination based on only two points in time, at which gape is 20% and 95% of maximal gape. Such a determination method may make TTPG more prone to measurement errors compared with $\Delta G/\Delta t$, which is based on averages over multiple time points (Fig. 1). Indeed, by excluding two apparent outliers (standard length=190, standard length=150), the scaling exponent of TTPG with standard length becomes 1.13±0.21, similar to the previously reported value.

As suggested by Day et al., in the present study, we present scaled flow speeds at the distance of $\frac{1}{2}$ gape distance from the mouth center (Day et al., 2005). This framework of scaling flow speed removes much of the variability in the data and facilitates the analysis of spatio-temporal flow patterns in front of different sized fish. However, gape size increases isometrically with standard length in bluegill, and the unscaled spatial patterns of flow speed change accordingly. If the gape size and the speed at the center of the mouth are known, the flow speed at any given point along the centerline extending out from the center of the mouth can be calculated. Since both gape size and peak flow speed increase in proportion to standard length, flow speed at any absolute distance from the mouth is expected to increase as a function of body length. That is, as bluegill grow, flow speed at a given distance in front of the mouth increases because that distance becomes relatively closer to the mouth, where speeds are higher, and because the fish is capable of higher induced flow speeds. This increase in induced flow speed performance on an absolute scale may be particularly important for diet shifts to larger prey types during ontogeny.

Although the connections have not yet been explicitly made between induced flow speed and more integrative measures of feeding performance, such as handling time or success rate, the increase in flow speed and closing speed on the prey during bluegill ontogeny suggests that these performance metrics are important to bluegill feeding ecology. Indeed, handling times of bluegill feeding on *Daphnia* and chironomids have been shown to decrease with body size (Mittelbach, 1981), which is expected if their ability to produce stronger suction flows improves with size. The increased closing speed can be important in capturing larger prey, as translational distance increases with body size in tail-flipping spiny lobsters (Nauen and Shadwick, 1999). However, transitional velocity did not change with increasing body size (Nauen and Shadwick, 1999). The observed increase in flow speed and closing speed on the prey with growth may also contribute to the ontogenetic habitat shift of bluegill from the highly vegetated littoral zones they inhabit at small size to the pelagic habitats they move to later on in their life cycle (Mittelbach, 1984). The diet of larger pelagic bluegill consists mostly of zooplankton (Mittelbach, 1984), for which high performance suction feeding may be an important adaptation.

The flow speed external to the mouth is an important metric of suction feeding performance, indicating the fish's ability to transfer force from the musculoskeletal system to the water around it. This study indicates that bluegill sunfish become higher-performance suction feeders as they grow. In the context of predator–prey interactions, the speed and acceleration of water external to the mouth are important in determining the forces exerted on the prey (Holzman et al., 2007; Van Wassenbergh et al., 2006a; Wainwright and Day, 2007). However, that force is a function of the spatio-temporal pattern of flow at the frame of reference of the prey, not of the predator. Therefore, strike accuracy, gape size, the closing speed on the prey and prey size will also contribute to strike success.

REFERENCES

Biewener, A. A. (1983). Allometry of quadrupedal locomotion-the scaling of duty factor, bone curvature and limb orientation to body size. *J. Exp. Biol.* **105**, 147-171.

Bishop, K. L., Wainwright, P. C. and Holzman, R. (in press). Anterior to posterior wave of buccal expansion in suction feeding fish is critical for optimizing fluid flow velocity profile. *J. R. Soc. Interface.* doi:10.1098/rsif.2008.0017

Brown, J. H. and West, G. B. (2000). *Scaling in Biology*. New York: Oxford University Press.

Carroll, A. M., Wainwright, P. C., Huskey, S. H., Collar, D. C. and Turingan, R. G. (2004). Morphology predicts suction feeding performance in centrarchid fishes. *J. Exp. Biol.* **207**, 3873-3881.

Collar, D. C. and Wainwright, P. C. (2006). Discordance between morphological and mechanical diversity in the feeding mechanism of centrarchid fishes. *Evolution* **60**, 2575-2584.

Day, S. W., Higham, T. E., Cheer, A. Y. and Wainwright, P. C. (2005). Spatial and temporal patterns of water flow generated by suction-feeding bluegill sunfish *Lepomis macrochirus* resolved by Particle Image Velocimetry. *J. Exp. Biol.* **208**, 2661-2671.

Drucker, E. G. and Jensen, J. S. (1996). Pectoral fin locomotion in the striped surfperch.2. Scaling swimming kinematics and performance at a gait transition. *J. Exp. Biol.* **199**, 2243-2252.

Ferry-Graham, L. A., Wainwright, P. C. and Lauder, G. V. (2003). Quantification of flow during suction feeding in bluegill sunfish. *Zoology (Jena)* **106**, 159-168.

Hendriks, A. J. (1999). Allometric scaling of rate, age and density parameters in ecological models. *Oikos* **86**, 293-310.

Herrel, A., Van Wassenbergh, S., Wouters, S., Adriaens, D. and Aerts, P. (2005). A functional morphological approach to the scaling of the feeding system in the African catfish, *Clarias gariepinus. J. Exp. Biol.* **208**, 2091-2102.

Higham, T. E., Day, S. W. and Wainwright, P. C. (2005). Sucking while swimming: evaluating the effects of ram speed on suction generation in bluegill sunfish *Lepomis macrochirus* using digital particle image velocimetry. *J. Exp. Biol.* **208**, 2653-2660.

Higham, T. E., Day, S. W. and Wainwright, P. C. (2006a). Multidimensional analysis of suction feeding performance in fishes: fluid speed, acceleration, strike accuracy and the ingested volume of water. *J. Exp. Biol.* **209**, 2713-2725.

Higham, T. E., Day, S. W. and Wainwright, P. C. (2006b). The pressures of suction feeding: the relation between buccal pressure and induced fluid speed in centrarchid fishes. *J. Exp. Biol.* **209**, 3281-3287.

Holzman, R., Day, S. W. and Wainwright, P. C. (2007). Timing is everything: coordination of strike kinematics affects the force exerted by suction feeding fish on attached prey. *J. Exp. Biol.* **210**, 3328-3336.

Johnson, J. B. and Omland, K. S. (2004). Model selection in ecology and evolution. *Trends Ecol. Evol. (Amst.)* **19**, 101-108.

Lauder, G. V. (1980). Hydrodynamics of prey capture in teleost fishes. In *Biofluid Mechanics*. Vol. 2 (ed. D. Schenck), pp. 161-181. New York: Plenum Press.

Magee, L. (1990). R2 measures based on Wald and likelihood ratio joint significance tests. *Am. Stat.* **44**, 250-253.

Mittelbach, G. G. (1981). Foraging efficiency and body size-a study of optimal diet and habitat use by bluegills. *Ecology* **62**, 1370-1386.

Mittelbach, G. G. (1984). Predation and resource partitioning in 2 sunfishes (Centrarchidae). *Ecology* **65**, 499-513.

Muller, M., Osse, J. W. M. and Verhagen, J. H. G. (1982). A quantitative hydrodynamical model of suction feeding in fish. *J. Theor. Biol.* **95**, 49-79.

Nauen, J. C. and Shadwick, R. E. (1999). The scaling of acceleratory aquatic locomotion: Body size and tail-flip performance of the California spiny lobster *Panulirus interruptus*. *J. Exp. Biol.* **202**, 3181-3193.

Peters, R. H. (1983). *The Ecological Implications of Body Size*. Cambridge: Cambridge University Press.

Pinheiro, J. C. and Bates, D. M. (2000). *Mixed-effects models in S and S-plus*. New York: Springer.

Raffel, M., Willert, C. E. and Kompenhans, J. (1998). *Particle Image Velocimetry: A Practical Guide*. Berlin: Springer.

Richard, B. A. and Wainwright, P. C. (1995). Scaling the feeding mechanism of Largemouth Bass (*Micropterus salmoides*)-kinematics of prey capture. *J. Exp. Biol.* **198**, 419-433.

Sanford, C. P. J. and Wainwright, P. C. (2002). Use of sonomicrometry demonstrates the link between prey capture kinematics and suction pressure in largemouth bass. *J. Exp. Biol.* **205**, 3445-3457.

Taylor, W. (1967). An enzyme method of clearing and staining small vertebrates. *Proc. US Natl. Mus.* **122**, 1-17.

van Leeuwen, J. L. and Muller, M. (1983). The recording and interpretation of pressures in prey-sucking fish. *Neth. J. Zool.* **33**, 425-475.

Van Wassenbergh, S., Aerts, P. and Herrel, A. (2005). Scaling of suction-feeding kinematics and dynamics in the African catfish, *Clarias gariepinus. J. Exp. Biol.* **208**, 2103-2114.

Van Wassenbergh, S., Aerts, P. and Herrel, A. (2006a). Hydrodynamic modelling of aquatic suction performance and intra-oral pressures: limitations for comparative studies. *J. R. Soc. Interface* **3**, 507-514.

Van Wassenbergh, S., Aerts, P. and Herrel, A. (2006b). Scaling of suction feeding performance in the catfish *Clarias gariepinus. Physiol. Biochem. Zool.* **79**, 43-56.

Van Wassenbergh, S., Herrel, A., James, R. S. and Aerts, P. (2007). Scaling of contractile properties of catfish feeding muscles. *J. Exp. Biol.* **210**, 1183-1193.

Wainwright, P. C. and Day, S. W. (2007). The forces exerted by aquatic suction feeders on their prey. *J. R. Soc. Interface* **4**, 553-560.

Wainwright, P. C. and Richard, B. A. (1995). Scaling the feeding mechanism of the Largemouth Bass (*Micropterus salmoides*)-motor pattern. *J. Exp. Biol.* **198**, 1161-1171.

Wainwright, P. C. and Shaw, S. S. (1999). Morphological basis of kinematic diversity in feeding sunfishes. *J. Exp. Biol.* **202**, 3101-3110.

Wainwright, P. C., Huskey, S. H., Turingan, R. G. and Carroll, A. M. (2006). Ontogeny of suction feeding capacity in snook, *Centropomus undecimalis. J. Exp. Zool.* **305A**, 246-252.

Wainwright, P. C., Carroll, A. M., Collar, D. C., Day, S. W., Higham, T. E. and Holzman, R. (2007). Suction feeding mechanics, performance, and diversity in fishes. *Integr. Comp. Biol.* **47**, 96-106.

Werner, E. E., Gilliam, J. F., Hall, D. J. and Mittelbach, G. G. (1983). An experimental test of the effects of predation risk on habitat use in fish. *Ecology* **64**, 1540-1548.

Westneat, M. W. (2006). Skull biomechanics and suction feeding in fishes. In *Fish Biomechanics* (ed. G. V. Lauder and R. E. Shadwick). San Diego: Elsevier Academic Press.